Supplementary figures to the manuscript:

Empirical Formula to Calculate Ionic Strength of Limnetic and Oligohaline Water on the Basis of Electric Conductivity: Implications for Limnological Monitoring

Michał Woszczyk [1,*], Alfred Stach [2], Jakub Nowosad [2], Izabela Zawiska [3], Katarzyna Bigus [4] and Monika Rzodkiewicz [1]

[1] Biogeochemistry Research Group, Adam Mickiewicz University, B. Krygowskiego 10, 61-680 Poznan, Poland
[2] Department of Geoinformation, Adam Mickiewicz University, B. Krygowskiego 10, 61-680 Poznan, Poland
[3] Past Landscapes Dynamics Laboratory, Institute of Geography and Spatial Organisation, Polish Academy of Sciences, Twarda 51/55, 00-818 Warsaw, Poland
[4] Department of Environmental Chemistry, Akademia Pomorska, Arciszewskiego 22a, 76-200 Slupsk, Poland
* Correspondence: woszczyk@amu.edu.pl; Tel.: +48-61-829-6194

submitted to *Water*

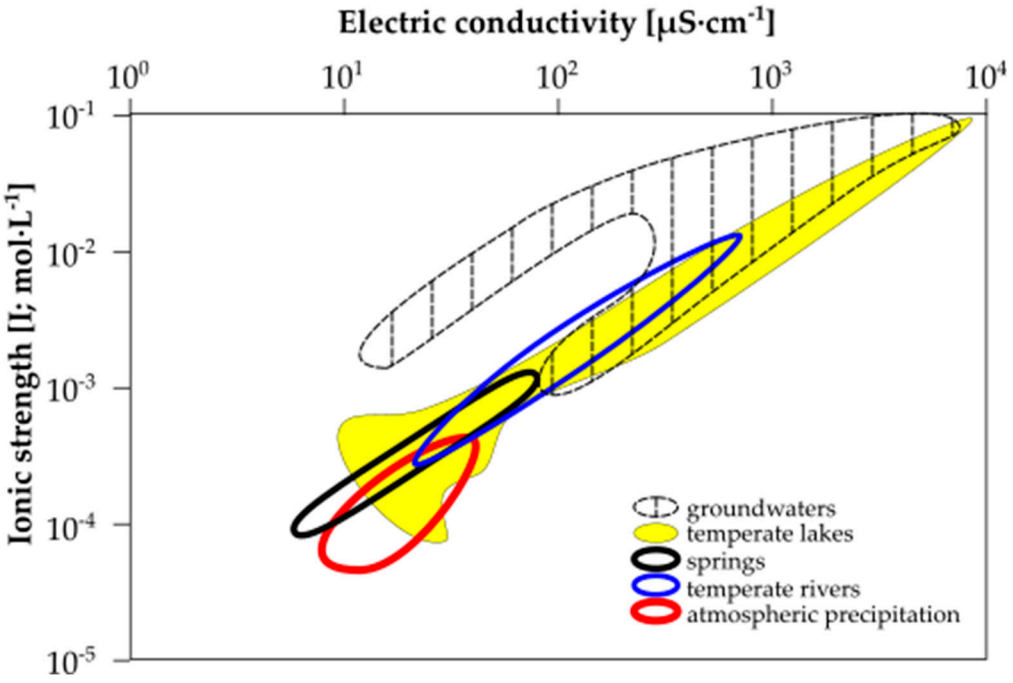

Figure S1. Electric conductivity (EC) vs ionic strength (I) in different types of fresh waters.

Note considerable variability in ground waters. The variability is determined by chemical composition of waters and makes it difficult to establish an universal empirical formula to derive I from *EC*. Ground water data from [53 - 56]. Lake water data from the databases of Leibniz Institute of Freshwater Ecology and Inland Fisheries (IGB Berlin, Germany) and Swiss Federal Institute of Aquatic Science and Technology (EAWAG, Kastanienbaum, Switzerland) as well as [57 - 58] and the authors' measurements. River water data from [59 - 62]. Spring water data from [61]. Rain water data from the Integrated Environmental Monitoring Base Station, Poland.

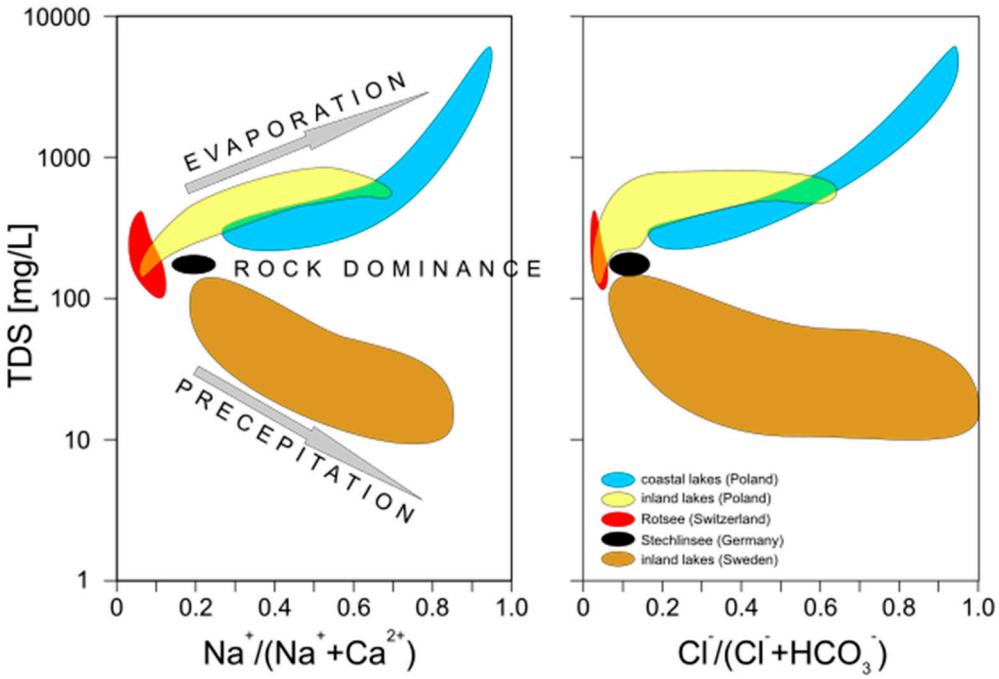

Figure S2. Chemical composition of water in the lakes of this study according to Gibbs.

Grey arrows indicate the increasing contribution from environmental factors (precipitation, evaporation and rock dominance) in controlling lake water chemistry. The lakes monitored represent all hydrochemical types of natural waters thus implying that the data used for model development are representative for all natural/seminatural temperate lakes.

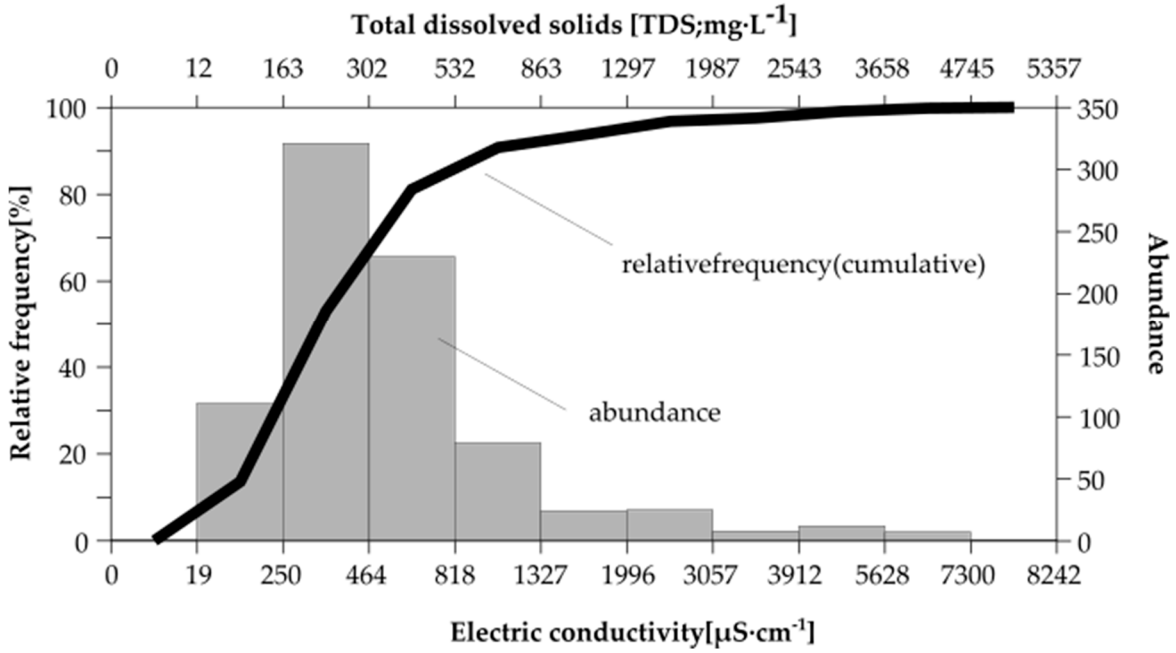

Figure S3. EC (and TDS) frequency distribution in a data base.

The distribution is highly positively skewed and records with EC between 250 and 818 were the most abundant. *EC* classes of the histogram were distinguished using Jenks optimization [63].

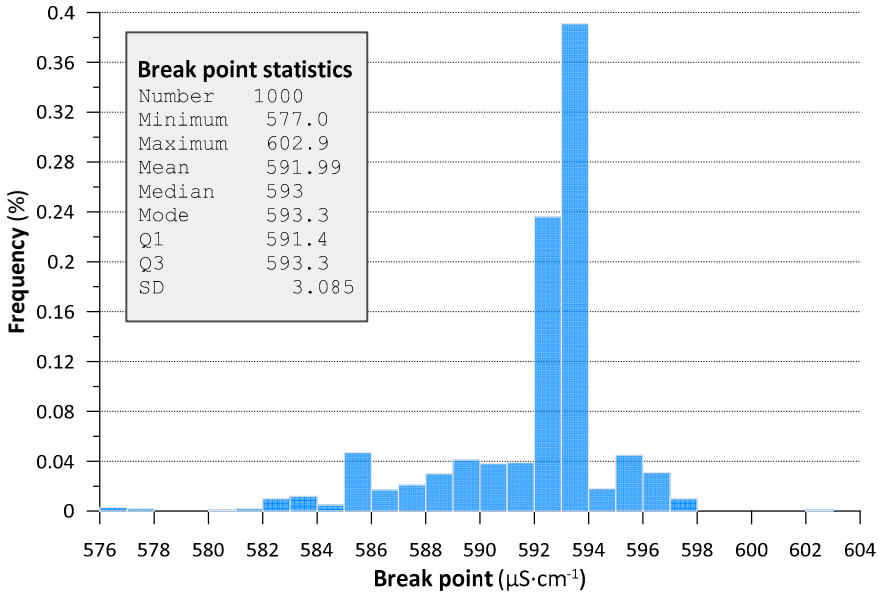

Figure S4. Histogram and descriptive statistics of the BP1 position in one breakpoint regression models obtained for 1000 random samples taken from original dataset.

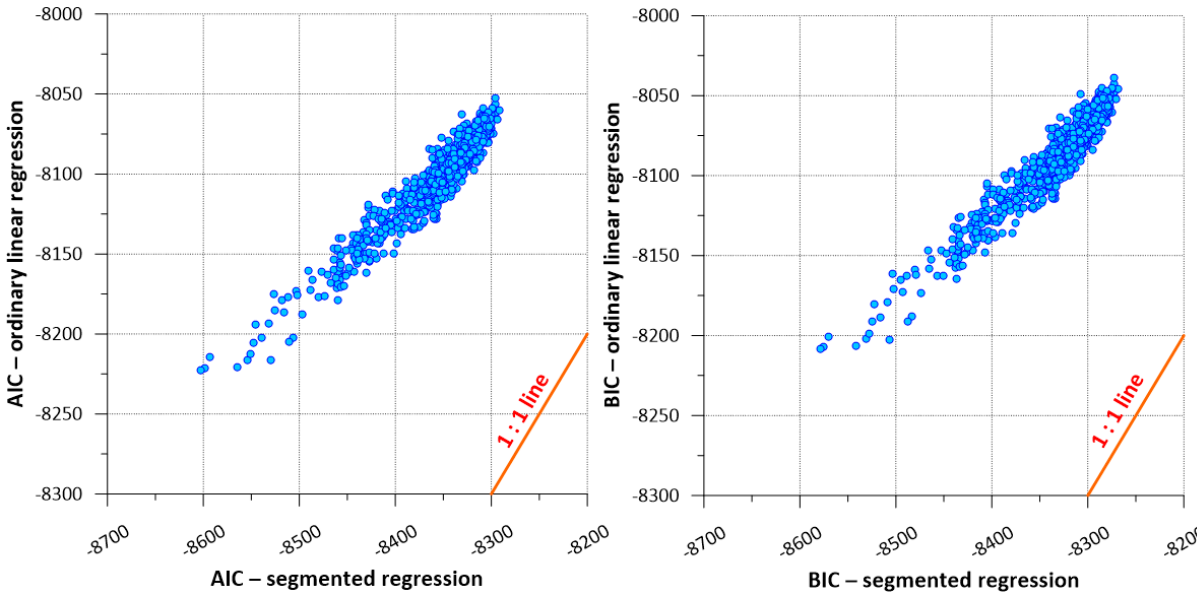

Figure S5. Relationship between the model fittings for segmented regression and ordinary linear regression in terms of Akaike information criterion (AIC; left panel) and Bayesian information criterion (BIC; right panel) calculated for 1000 random subsamples from EC vs I database.

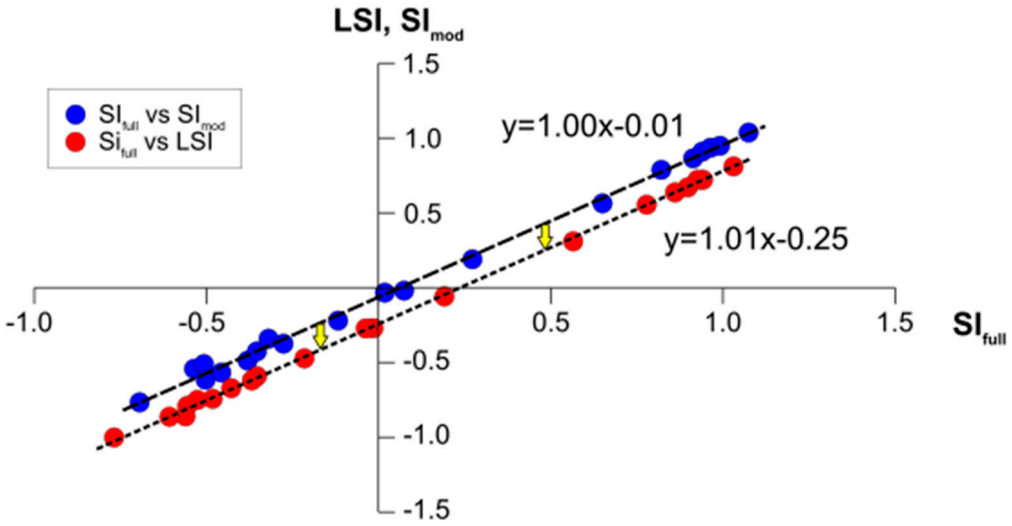

Figure S6. The application of the model developed for calculating saturation index for carbonates in lake waters.

The SI calculated using our modelled γ ion activity coefficients (SI_{model}) and Langelier SI (LSI) computed with an online LSI calculator were compared to SI calculated on the basis of full ion composition of Lake Kierskie waters (SI_{full}). Both methods reproduced SI_{full} with considerable accuracy, however, SI_{model} showed better agreement with the empirical data. There were systematic differences between SI_{full} and SI_{model} as well as LSI of c.a. -0.06 and c.a. -0.24, respectively.

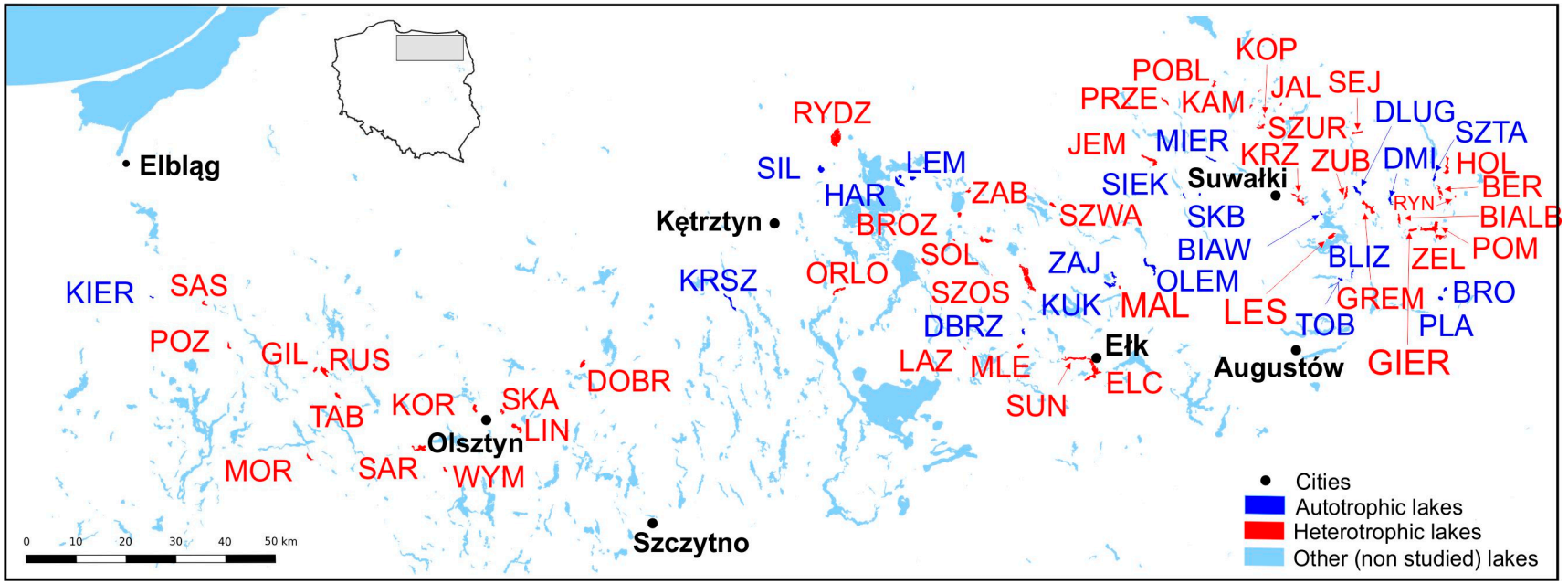

Figure S7. The results of screening of ΔpCO_2 (difference between pCO_2 in lake surface waters and atmospheric CO_2 concentration) for lakes of NE Poland.

Heterotrophic lakes showed positive ΔpCO_2 (emitted CO_2 to the atmosphere) while autotrophic lakes had negative ΔpCO_2 values (absorbed CO_2 from the atmosphere). The map of lakes taken from [64].

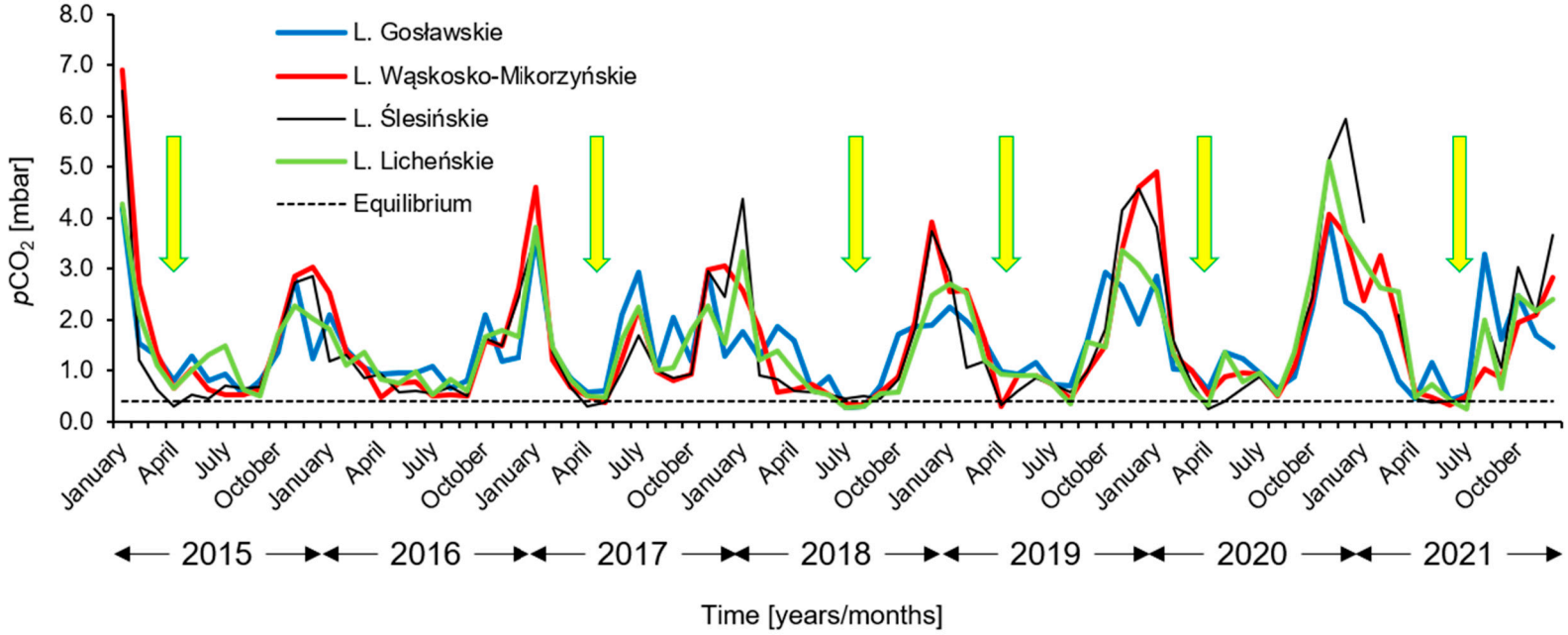

Figure S8. Temporal changes in pCO_2 in the surface waters of the Konin lakes between January 2015 and December 2021. Yellow arrows indicate periods of autotrophy (i.e. when pCO_2 < equilibrium pCO_2.

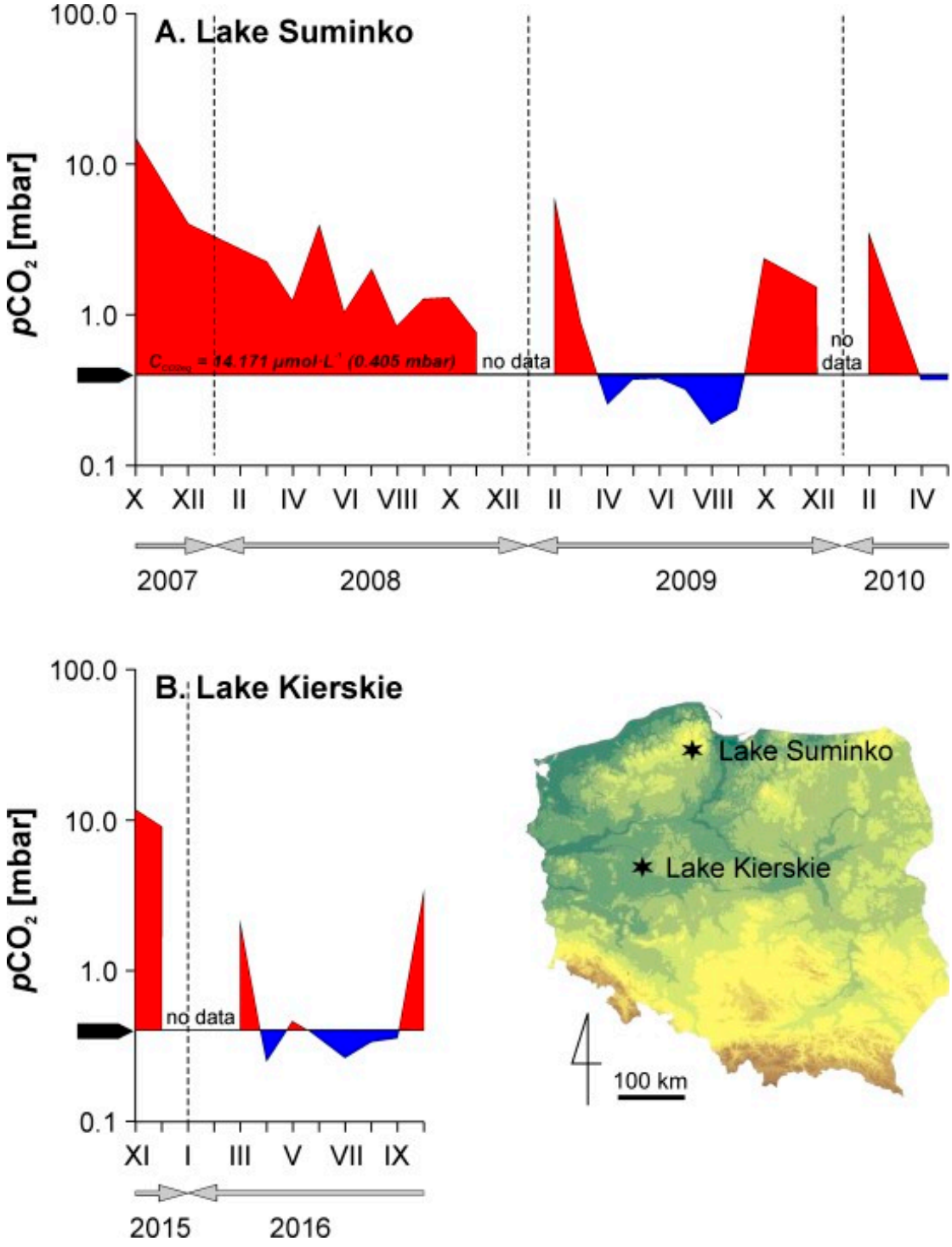

Figure S9. Temporal changes in pCO_2 in the surface waters of Lake Suminko (A) and Lake Kierskie (B).

Arrow indicate equilibrium CO_2 concentration in Polish lakes. Heterotrophic periods marked in red, while autotrophic in blue.

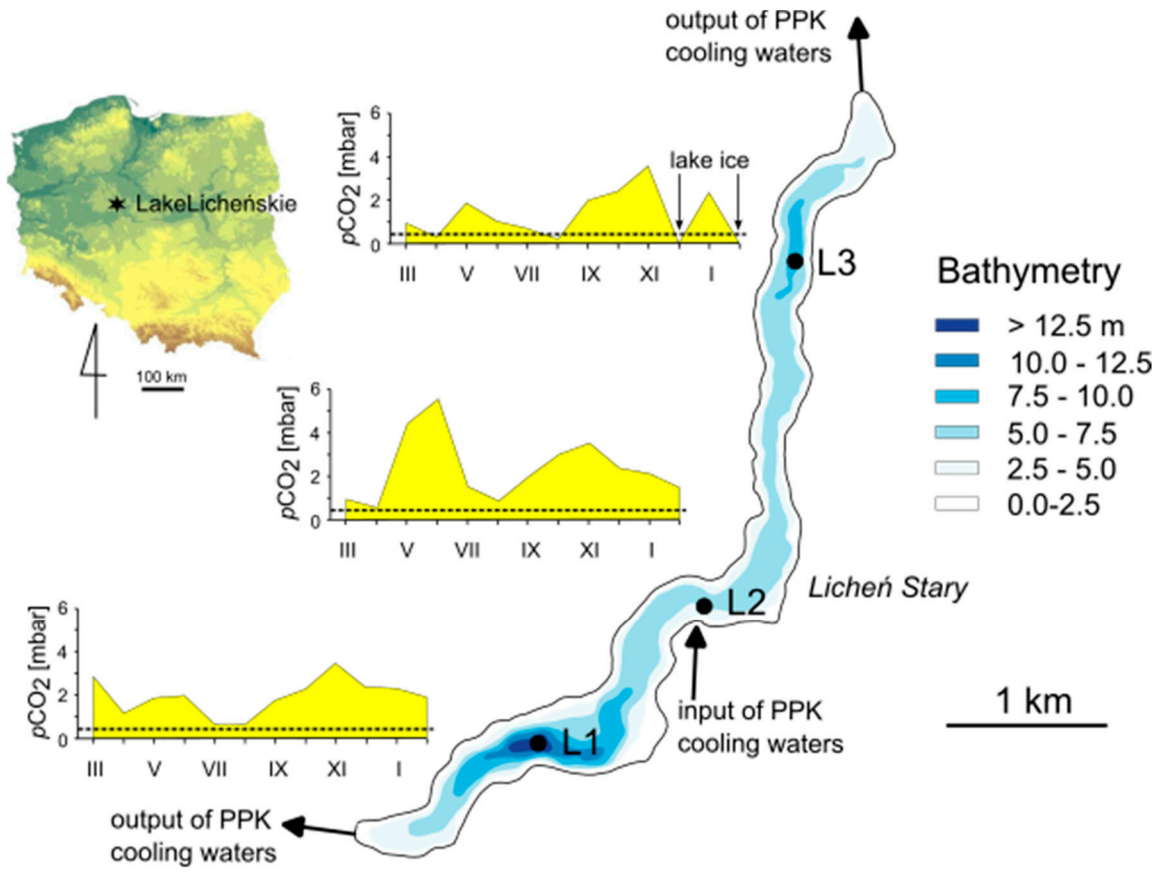

Figure S10. Spatial and temporal changes in pCO_2 in the surface water of Lake Licheńskie. the equilibrium CO_2 concentrations in Polish lakes marked with a dotted line.

The data enabled identifying CO_2 emission hotspot. Bathymetric map according to Inland Fisheries Institute, Olsztyn, PL.

Table S1. Location of data collection sites, sampling strategy and data availability

No.	Lake	Country[#]	Coordinates	Lake type[&]	EC [μS·cm^{-1}]	Data collection period and frequency	Source & availability
1	Licheńskie	PL	52°18′30″N, 18°20′19″E	GL	566 – 687	Data collected at the deepest point every 1 m from the surface to the bottom, between 12.2014 and 09.2015 with monthly resolution	Unpublished; available on request at Biogeochemistry Research Group, AMU Poznań, PL
2	Dębno	PL	52°17′31″N, 16°42′09″E	GL	818 – 1140	Data collected at the deepest point every 1 m from the surface to the bottom between 07.2019 and 07.2020 with monthly resolution	Unpublished; available on request at Biogeochemistry Research Group, AMU Poznań, PL
2	Łódzko-Dymaczewskie	PL	52°15′22″N, 16°44′31″E	GL	570 – 815		
4	Trześniowskie (Ciecz)	PL	52°20′50″N, 15°17′26″E	GL	358 – 473		
5	Ostrowite	PL	53°48′27″N, 17°36′16″E	GL	224 – 226	Data collected on 07-08.08.2017 at the deepest points on the lakes 1 m below the lake surface	[57]
6	Jeleń	PL	53°49'37"N, 17°35'37"E	GL	231		
7	Płęsno	PL	53°48'52"N, 17°32'57"E	GL	253		
8	Krzywce Wielkie	PL	53°50'18"N, 17°33'37"E	GL	42.3		
9	Zielone	PL	53°49'18"N, 17°35'49"E	GL	238		
10	Skrzynka	PL	53°48'52"N, 17°31'30"E	GL	241		
11	Krzywce Małe	PL	53°49'32"N, 17°32'43"E	GL	44.2		
12	Mielnica	PL	53°48'25"N, 17°31'05"E	GL	269		
13	Główka	PL	53°48'36"N, 17°34'16"E	GL	234		
14	Bełczak	PL	53°48'53"N, 17°34'23"E	GL	226		
15	Resko Przym.	PL	54°08′32″N, 15°22′37″E	CL	4927 – 7087	Data collected from surface and near-bottom layer between 02.2015 and 10.2015 with quarterly resolution	Unpublished; available on request at Biogeochemistry Research Group, AMU Poznań, PL
16	Jamno	PL	54°16′24″N, 16°09′02″E	CL	407 – 521		
17	Bukowo	PL	54°20′35″N, 16°16′43″E	CL	1394 – 2770		
18	Kopań	PL	54°29′04″N, 16°27′02″E	CL	2602 – 2966		
19	Wicko	PL	54°32′22″N, 16°37′08″E	CL	376 – 625		
20	Gardno	PL	54°39′14″N, 17°06′43″E	CL	1455 – 3057		
21	Łebsko	PL	54°42′22″N, 17°23′01″E	CL	3618 – 8242		
22	Sarbsko	PL	54°45′58″N, 17°38′10″E	CL	374 – 1327	Data collected from surface and near-bottom layer between 12.2007 and 08.2008 with quarterly resolution	[65 - 66]
23	Stechlin	DE	53°09′00″N, 13°01′30″E	GL	251 – 284	Data collected at the deepest point from the surface to the bottom between 01.2020 and 12.2021 with monthly resolution	Data available on request at the IGB data repository (https://fred.igb-berlin.de)

24	Rotsee	CH	47°04′11″N, 8°18′51″E	GL	182 – 580	Data collected at the deepest point from the surface to the bottom between 02.2007 and 01.2008 with monthly resolution	[67]
25	Edasjön	SV	59°48'06"N, 17°53'57"E	GL	73 – 201	Data collected at the lake surface monthly between 1983 and 2022	Data available at https://miljodata.slu.se/MVM; [58]
26	Siggeforasjön	SV	59°58'36"N, 17°08'41"E	GL	41 – 55		
27	Fiolen	SV	57°05'03"N, 14°31'51"E	GL	65 – 66		
28	Tångerdasjön	SV	57°27'43"N, 15°03'54"E	GL	65 – 158		

[#]Country: PL – Poland, DE – Germany, CH – Switzerland, SV – Sweden

[&]Lake type: CL – coastal lake, GL – glacial lake

Table S2. Activity coefficient γ for HCO_3^- for different *EC* and *t*

t	*EC* [µS·cm^{-1}]					
[°C]	50	100	500	1000	5000	8000
0	0.972	0.960	0.916	0.893	0.816	0.786
10	0.972	0.959	0.915	0.892	0.813	0.783
20	0.971	0.958	0.913	0.890	0.811	0.780
30	0.971	0.958	0.912	0.889	0.808	0.778

Table S3. Activity coefficient γ for CO_3^- for different *EC* and *t*

t	*EC* [µS·cm^{-1}]					
[°C]	50	100	500	1000	5000	8000
0	0.893	0.851	0.707	0.642	0.454	0.39
10	0.891	0.848	0.703	0.637	0.448	0.39
20	0.890	0.846	0.699	0.633	0.443	0.38
30	0.888	0.844	0.695	0.628	0.438	0.38

Table S4. Activity coefficient γ for Ca^{2+} for different *EC* and *t*

t	*EC* [µS·cm^{-1}]					
[°C]	50	100	500	1000	5000	8000
0	0.894	0.853	0.716	0.655	0.483	0.429
10	0.893	0.851	0.712	0.650	0.477	0.424
20	0.891	0.848	0.709	0.646	0.472	0.419
30	0.889	0.846	0.705	0.642	0.467	0.414

Table S5. Activity coefficient γ for Mg^{2+} for different *EC* and *t*

t	*EC* [µS·cm^{-1}]					
[°C]	50	100	500	1000	5000	8000
0	0.896	0.856	0.727	0.671	0.517	0.471
10	0.894	0.854	0.723	0.667	0.512	0.466
20	0.893	0.852	0.720	0.663	0.507	0.461
30	0.891	0.850	0.716	0.659	0.503	0.456